Area of Macromolecular Complexes from the Ministry of Education, Science, and Culture, Japan.

Registry No. (CMe₃Li)(MEO₇) (copolymer), 118400-61-6; $H_2C=C(CH_3)CO_2(CH_2CH_2O)_3CH_2CO_2Li$ (homopolymer), 118400-50-3; $H_2C=C(CH_3)CO_2(CH_2CH_2O)_3CH_2CO_2K$ (homopolymer), 118400-52-5; $H_2C=C(CH_3)CO_2(CH_2CH_2O)_3CH_2CO_2Na$ (homopolymer), 118400-54-7; $H_2C=C(CH_3)CO_2(CH_2CH_2O)_7CH_2CO_2Li$ (homopolymer), 118400-56-9; $H_2C=C(CH_3)CO_2(CH_2CH_2O)_7CH_2CO_2K$ (homopolymer), 118400-58-1; $H_2C=C(CH_3)CO_2(CH_2CH_2O)_7CH_2CO_2Na$ (homopolymer), 118400-60-5; CME₃H, 118457-79-7.

References and Notes

(1) Wright, P. V. *Br. Polym. J.* **1975**, *319*, 137.
(2) Papke, B. L.; Ratner, M. A.; Shriver, D. F. *J. Phys. Chem. Solid* **1981**, *42*, 493.
(3) Berthier, C.; Gorecki, W.; Minier, M.; Armand, M. B.; Chabagno, J. M.; Riguad, P. *Solid State Ionics* **1983**, *11*, 91.
(4) Dupon, R.; Papke, B. L.; Ratner, M. A.; Whitmore, D. H.; Shriver, D. F. *J. Am. Chem. Soc.* **1982**, *104*, 6247.
(5) Weston, J. E.; Steel, B. C. H. *Solid State Ionics* **1982**, *7*, 81.
(6) Killes, A.; Le Nest, J. F.; Gandini, A.; Cheradame, H. *Macromolecules* **1984**, *17*, 63.
(7) Watanabe, M.; Ikeda, J.; Shinohara, I. *Polym. J.* **1983**, *15*, 65, 175.
(8) Yang, L. L.; McGhie, A. R.; Farrington, G. C. *J. Electrochem. Soc.* **1986**, *133*, 1380.
(9) Tsuchida, E.; Ohno, H.; Tsunemi, K.; Kobayashi, N. *Solid State Ionics* **1983**, *11*, 227.
(10) Kobayashi, N.; Uchiyama, M.; Shigehara, K.; Tsuchida, E. *J. Phys. Chem.* **1985**, *89*, 987.
(11) Kobayashi, N.; Ohno, H.; Tsuchida, E. *J. Chem. Soc. Jpn.* **1986**, 441.
(12) Kobayashi, N.; Ohno, H.; Tsuchida, E.; Hirohashi, R. *Koubunshi Ronbunshu* **1987**, *44*, 317.
(13) Blonsky, P. M.; Shriver, D. F.; Austin, P.; Allcock, H. R. *J. Am. Chem. Soc.* **1984**, *106*, 6854.
(14) Bannister, D. J.; Davies, G. R.; Word, I. M.; McIntyre, J. E. *Polymer* **1984**, *25*, 1600.
(15) Xia, D. W.; Soltz, D.; Smid, J. *Solid State Ionics* **1984**, *14*, 85.
(16) Le Mehaute, A.; Crepy, G.; Marcellin, G.; Hamaide, T.; Guyot, A. *Polym. Bull.* **1985**, *14*, 233.
(17) Bannister, D. J.; Davies, G. R.; Word, I. M.; McIntyre, J. E. *Polymer* **1984**, *25*, 1291.
(18) Hardy, L. C.; Shriver, D. F. *J. Am. Chem. Soc.* **1985**, *107*, 3823.
(19) Kobayashi, N.; Uchiyama, M.; Tsuchida, E. *Solid State Ionics* **1985**, *17*, 307.
(20) Kobayashi, N.; Hamada, T.; Ohno, H.; Tsuchida, E. *Polym. J.* **1986**, *18*, 661.
(21) Tsuchida, E.; Kobayashi, N.; Ohno, H. *Macromolecules* **1988**, *21*, 96.
(22) Cole, K. S.; Cole, R. H. *J. Chem. Phys.* **1941**, *9*, 341.
(23) Williams, M. L.; Landel, R. F.; Ferry, J. D. *J. Am. Chem. Soc.* **1955**, *77*, 3701.
(24) (a) Vogel, H. *Phys. Z.* **1921**, *22*, 645. (b) Tammann, V. G.; Hesse, W. Z. *Anorg. Allg. Chem.* **1926**, *156*, 245. (c) Fulcher, G. C. *J. Am. Ceram. Soc.* **1925**, *8*, 339.
(25) Wintersgill, M. C.; Fontanella, J. J.; Smith, M. K.; Greenbaum, S. G.; Adamic, K. J.; Andeen, C. G. *Polymer* **1987**, *28*, 633 and references therein.

Partition Coefficients of Rigid, Planar Multisubunit Complexes in Cylindrical Pores

Ruth E. Baltus

Department of Chemical Engineering, Clarkson University, Potsdam, New York 13676.
Received July 25, 1988; Revised Manuscript Received September 20, 1988

ABSTRACT: A theoretical investigation of the equilibrium partition coefficient of planar multisubunit model structures in cylindrical pores was undertaken. These models are rigid complexes assembled from identical spherical subunits. Model structures containing two to eight subunits were investigated. The effective hydrodynamic radius was found to reasonably characterize the partitioning properties of the multisubunit models; however, the partition coefficient for each multisubunit structure was significantly smaller than that for a spherical solute with the same hydrodynamic radius. The partitioning characteristics of the multisubunit complexes were comparable to those predicted for oblate ellipsoid particles with an axial ratio of ~0.01–0.05, a ratio which is considerably smaller than the ratio of the smallest to largest dimension of these structures. The results show that the partition coefficient does not correlate well with molecular radius, which is defined as the radius of a sphere with the same volume as the multisubunit complex.

Introduction

When the size of a solute is comparable to the pore size through which it is diffusing, reduced diffusion rates are observed. This phenomenon is called hindered diffusion and results from the combination of two effects: one is an equilibrium effect and the other a transport effect. The equilibrium partitioning of solute molecules between the pore and bulk solutions results in an intrapore concentration driving force which is less than the driving force based on bulk solution concentrations. The proximity of the pore wall causes an increase in the frictional resistance experienced by the solute as it diffuses through the pore. This description of the physics governing hindered diffusion becomes more complicated when one includes the influence of long-range solute–pore wall interactions. An understanding of the equilibrium and transport properties of macromolecules in porous media is important in applications such as size exclusion chromatography, membrane separation processes, and heterogeneous catalysis.

The equilibrium partitioning of solute molecules between pore and bulk solutions is described by using a partition coefficient, defined as the ratio of pore to bulk solution concentrations. A general expression for the partition coefficient, K, for rigid molecules based on statistical mechanics is[1]

$$K = \frac{C_p}{C_b} = \frac{\int_x \int_\Psi \exp[-E(x,\Psi)/kT]\, dx\, d\Psi}{\int_x \int_\Psi dx\, d\Psi} \quad (1)$$

where C_p is the solute concentration in the pore and C_b is the solute concentration in the bulk solution. Here, x and Ψ represent generalized position and molecular orientation coordinates, respectively. The potential energy of a solute molecule in the pore is represented by $E(x,\Psi)$; $E = 0$ in bulk solution.

Giddings et al.[1] evaluated the integrals in eq 1 for rigid molecules limited to steric or "hard-wall" interactions with the pore wall. This hard-wall potential field results in E

= 0 for $(\mathbf{x},\Psi)$ values where the solute boundaries do not overlap with the pore wall and $E = \infty$ for $(\mathbf{x},\Psi)$ values where the solute overlaps the pore wall. This leads to a discontinuous function for the Boltzmann factor, $\exp[-E(\mathbf{x},\Psi)/kT]$; this factor has a value of 1 when the solute does not overlap the pore wall and a value of 0 otherwise. For spherical solutes, the potential energy is independent of molecular orientation. Evaluation of the remaining position integrals in eq 1 is straightforward and leads to

$$K = \left(1 - \frac{a_s}{r_0}\right)^2 \qquad (2)$$

where a_s is the solute radius and r_0 is the pore radius. Equation 2 shows K to be simply the ratio of the area of two circles, one of radius $= r_0 - a_s$ and the other of radius $= r_0$.

For nonspherical molecules, the orientation integral in eq 1 can be expressed in terms of the Eulerian angles of a coordinate system whose origin is at the center of the solute molecule. However, the resulting integrals cannot be evaluated analytically, even for molecules with rotational symmetry. Numerical integration was used by Giddings et al.[1] to determine the partition coefficient for prolate ellipsoids in cylindrical and rectangular pores. These results were then used to investigate the relationship between the partition coefficient and various molecular size parameters. It was shown that the mean external length better characterizes partitioning than other size parameters such as radius of gyration, hydrodynamic radius, and molecular weight. The mean external length, also called the mean projected length, is twice the minimum distance between the center of the molecule and a flat surface, averaged over all orientations. The argument is made, and is substantiated with results for prolate ellipsoids, that two molecules with the same mean projected length will have similar partitioning characteristics regardless of their molecular conformation. The concept of the mean projected length as a characteristic parameter for partitioning of random coil polymers was discussed by Casassa.[2]

When the solute molecule is not rigid, integrals over molecular conformation must also be included in the numerator and denominator in eq 1. This problem was undertaken by Davidson et al.[3] for flexible linear macromolecules using a Monte Carlo technique. The results from this study illustrated the importance of molecular conformation on partitioning, showing that K for a linear polymer is smaller than K for a rigid sphere with the same ratio of hydrodynamic radius to pore radius.

The effect of electrostatic interactions between solute and pore wall has been considered by Smith and Deen.[4-6] The potential energy of interaction between a charged spherical solute and a charged pore wall was determined by solving the Poisson–Boltzmann equation for $E(\mathbf{x})$. Here, E is independent of orientation because calculations were limited to spherical molecules with uniformly distributed charge. The Boltzmann factor was determined at a number of radial positions, and the position integral in eq 1 was evaluated numerically. These results showed that electrostatic interactions can have a significant effect on the partition coefficient, predicting $K > 1$ for certain conditions.

For the past several years, efforts in our laboratory have been directed toward elucidating the macroscopic structure of oil residual fractions by using intrinsic viscosity and diffusion coefficient measurements.[7,8] The motivation for this work is the recognition that diffusional resistances can be significant in the catalytic processing of heavy oil
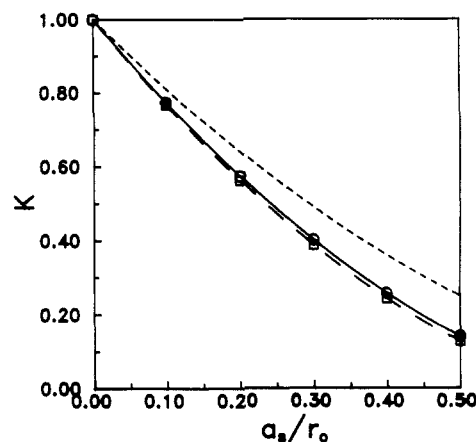
Figure 1. Partition coefficient values as a function of the ratio of hydrodynamic radius to pore radius: O, three-unit complex; □, eight-unit complex; —, polynomial fit to results for three-unit complex; – –, polynomial fit to results for eight-unit complex; - - -, spherical solute (eq 2).

feedstocks. The design and development of effective porous catalysts for such materials requires an understanding of the transport characteristics of these materials in small pores, and knowledge of the macromolecular shape or conformation is necessary for the prediction of reactant diffusion rates in small pores. An understanding of the equilibrium properties of these materials in small pores is also important in the interpretation of information obtained from size exclusion chromatography, a commonly used analytical technique in studies with petroleum-derived materials. On the basis of our experimental results, we have proposed model multisubunit structures to describe the macroscopic properties of Cold Lake bitumen vacuum bottoms. These models are rigid structures assembled from identical spherical subunits as shown in Figure 1. The theoretical predictions of Garcia de la Torre and Bloomfield[9] for intrinsic viscosity and frictional coefficient for these structures were used in interpreting the experimental results. In this paper, results from a theoretical investigation of the equilibrium partitioning of multisubunit complexes between pore and bulk solution are presented. These calculations have been limited to models with a planar geometry because our interest is in understanding the properties of petroleum-derived materials. These materials are comprised of aromatic and cyclic layers, and this it is expected that planar models will reasonably describe their behavior. The approach presented here could also be applied to multisubunit structures with other geometries.

Partition Coefficient Calculations

The partition coefficient for each model structure is determined by evaluating the integrals in eq 1 over position and orientation space. The pore is considered to be a capillary with constant radius and length much greater than its radius. Only steric or hard-wall interactions between the solute molecule and the pore wall are considered. Therefore, the Boltzmann factor $\exp[-E(\mathbf{x},\Psi)/kT]$ is limited to values of 1 or 0. We define $P(\mathbf{x})$ to be the time-averaged or ensemble average probability of finding a solute molecule at position $\mathbf{x}$ in the pore. $P(\mathbf{x})$ is defined by considering the integral over orientation space at fixed position:

$$\int_{\Psi} \exp\left(\frac{-E(\mathbf{x},\Psi)}{kT}\right) d\Psi = P(\mathbf{x}) \qquad (3)$$

The coordinate Ψ is normalized such that $\int_{\Psi} P \, d\Psi = 1$ in

$$A = \begin{bmatrix} \cos\psi\cos\phi - \cos\theta\sin\phi\sin\psi & -\sin\psi\cos\phi - \cos\theta\sin\phi\cos\psi & \sin\theta\sin\phi \\ \cos\psi\sin\phi + \cos\theta\cos\phi\sin\psi & -\sin\psi\sin\phi + \cos\theta\cos\phi\cos\psi & -\sin\theta\cos\phi \\ \sin\theta\sin\psi & \sin\theta\cos\psi & \cos\theta \end{bmatrix} \quad (6)$$

bulk solution (i.e., when $K = 1$). As noted by Giddings et al.,[1] $P(\mathbf{x})$ can also be considered to be the fraction of allowed orientations at position $\mathbf{x}$. An allowed orientation is one in which the solute molecule does not intersect the pore wall. This definition of $P(\mathbf{x})$ is the basis for the calculations presented here.

A cylindrical coordinate system (r,α,z) with origin at the pore center is used to describe the position of the model structure in the pore. The potential energy, E, is independent of α and z; therefore, the position integral reduces to an integral over the radial coordinate, r. Equation 1 then reduces to

$$K = \frac{C_p}{C_b} = \frac{\int_{\mathbf{x}} P(\mathbf{x})\,d\mathbf{x}}{\int_{\mathbf{x}} d\mathbf{x}} = \frac{\int_0^1 P(\beta)\beta\,d\beta}{\int_0^1 \beta\,d\beta} \quad (4)$$

where β is the radial coordinate, normalized with respect to the pore radius. In order to evaluate the integral in eq 3, another coordinate system fixed to the molecule is defined by using $\mathbf{x}_p = (x_p, y_p, z_p)$. This coordinate system is related to coordinates $\mathbf{x} = (x,y,z)$ fixed in the fluid by using the Eulerian angles (ψ,ϕ,θ). The two coordinate systems are related through the following transformation:[10]

$$\mathbf{x} = A \cdot \mathbf{x}_p \quad (5)$$
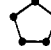
with matrix A given in eq 6.

The origin of coordinates $\mathbf{x}_p$ was chosen to be the center of mass of the structure. The coordinates of each subunit, $x_p(i)$, $y_p(i)$, and $z_p(i)$ were then defined from the geometry of the structure (Figure 1). To determine $P(\beta)$, the structure was positioned in the pore and rotated through the angles ψ, ϕ, and θ in increments of $\pi/20$. At each orientation, the position of each subunit in the pore was determined by using the transformation in eq 5 and 6. If each subunit fell within the bounds of the pore, the orientation was allowed; otherwise it was not. The ratio of allowed orientations relative to the total number of orientations investigated was calculated, and this ratio is simply the value $P(\beta)$. This calculation was repeated for 100 equally spaced radial positions within the pore, providing discrete values of $P(\beta)$ versus β. The values of $P(\beta)$ were then interpolated by using a cubic spline routine. The partition coefficient was determined by evaluating the integral in eq 4 with the cubic spline interpolant and an adaptive integration scheme which utilizes a 21-point Gauss–Kronrod rule. The cubic spline and integration routines were from the IMSL library. All computations were performed on Clarkson's Alliant FX/8 computer.

Results and Discussion

In reporting the results from this investigation, two solute size parameters are considered. The first is the effective hydrodynamic radius of each structure, which can be determined from the frictional coefficient. The second size parameter is the molecular radius. This is the radius of a sphere with the same volume as the model. In comparing results for each structure, the solute size is normalized with respect to the pore radius, r_0. Calculations were performed for each geometry for $a_s/r_0 = 0.1, 0.2, 0.3, 0.4$, and 0.5.

The results by Garcia de la Torre and Bloomfield[9] for the translation of these multisubunit structures in bulk solution were reported for each structure in terms of the

Table I
Model Structures and Predictions for Friction Factor[a,9]

structure	$f/(6\pi\mu\sigma)$	structure	$f/(6\pi\mu\sigma)$
(octagon)	2.543	(square)	1.700
		(triangle)	1.509
(hexagon)	2.129	(dumbbell)	1.333
(pentagon)	1.922		

[a] Each circle represents the center of a spherical subunit of radius σ; each line segment has length 2σ.

dimensionless ratio $f/(6\pi\mu\sigma)$, where f is the frictional coefficient, μ is the solvent viscosity, and σ is the radius of each subunit in the structure. The effective hydrodynamic radius a_s is related to the frictional coefficient through Stokes' law, and therefore

$$a_s = \frac{f}{6\pi\mu\sigma}\sigma \quad (7)$$

The value of $f/(6\pi\mu\sigma)$ for each structure is listed in Table I.

The results for the models with three and eight subunits are presented in Figure 1 as a plot of K versus a_s/r_0. Also included in this figure are the predictions for a spherical molecule (eq 2). The results for the other geometries are in close agreement with the values shown in Figure 1, with K for the models with four, five, and six subunits falling between the values for the two structures included in the figure. Figure 1 shows that there is only a small difference between the value of K predicted for the three- and eight-unit complexes with the same value of a_s/r_0. As expected, this difference increases as the ratio a_s/r_0 increases. Figure 1 also shows that there is a significant difference between the partition coefficient values predicted for a spherical solute when compared to the multisubunit structures. For $a_s/r_0 = 0.5$, K for the sphere is almost twice the value for the eight-unit complex. A value of $a_s/r_0 = 0.2$ is characteristic of the reactant to pore size ratio in a heavy oil processing catalyst. The ratio of solute to pore size in size exclusion chromatography can span the range of size ratios presented in Figure 1. The results in Figure 1 demonstrate that significant errors can be introduced if one assumes equilibrium properties of a spherical solute are representative of the properties of more planar molecules.

The values presented in Figure 1 as K versus a_s/r_0 have been replotted in Figure 2 as K versus the ratio r^*/r_0, where r^* is the molecular radius of the solute. For each structure

$$r^* = (n\sigma^3)^{1/3} \quad (8)$$

where n is the number of subunits in the structure. Figure 2 shows that there is a poor correlation between K and r^*/r_0 for these structures. Figures 1 and 2 illustrate the importance of recognizing the difference in the various size parameters that one can use in describing molecular size. The hydrodynamic radius provides a reasonable correlation between K and molecular size for the planar multisubunit structures. However, a poor correlation is observed when
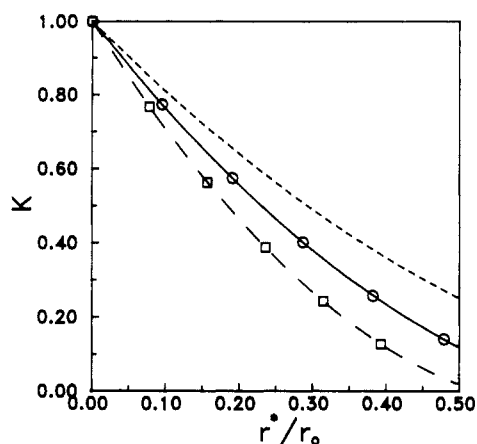
Figure 2. Partition coefficient values as a function of the ratio of molecular radius to pore radius: O, three-unit complex; □, eight-unit complex; —, polynomial fit to results for three-unit complex; – –, polynomial fit to results for eight-unit complex; - - -, spherical solute (eq 2).

Table II
Comparison of Partition Coefficients for Multisubunit Complexes

no. of subunits	a_s/r_0		$r*/r_0{}^a$	
	0.2	0.5	0.2	0.5
1	0.640	0.250	0.640	0.250
2	0.586	0.152	0.564	0.121
3	0.574	0.142	0.556	0.119
4	0.568	0.135	0.537	0.098
5	0.569	0.136	0.519	0.077
6	0.566	0.133	0.503	0.056
8	0.563	0.129	0.464	0.018

^{a} Predicted by using polynomial fit (eq 9 and Table III).

Table III
Coefficients for Second-Order Polynomial Fit (Eq 9)

no. of subunits	$\lambda = a_s/r_0$			$\lambda = r*/r_0$		
	a	b	c	a	b	c
2	1.000	−2.322	1.249	1.000	−2.457	1.399
3	1.000	−2.408	1.379	1.000	−2.524	1.522
4	1.000	−2.464	1.442	1.000	−2.654	1.702
5	1.000	−2.472	1.475	1.000	−2.778	1.863
6	1.000	−2.462	1.452	1.000	−2.885	1.993
8	1.000	−2.486	1.480	1.000	−3.160	2.393

one compares the multisubunit structures to a sphere with the same value of a_s/r_0. In contrast, the molecular radius does not characterize the partitioning behavior even when one compares the various multisubunit structures. The partition coefficient values for each model geometry are listed in Table II.

The five values of K for each structure were fitted to second-order polynomials

$$K = a + b\lambda + c\lambda^2 \qquad (9)$$

where λ is either a_s/r_0 or $r*/r_0$. The values of the coefficients a, b, and c are listed in Table III. In all cases, an excellent fit was observed.

One might expect that the partitioning characteristics of the planar complexes would be similar to those for an oblate ellipsoid of revolution. To provide a comparison, the partition coefficient for an oblate ellipsoid was determined by using an expression presented by Giddings et al.[1] for the mean projected length of oblate ellipsoids as a function of axial ratio. By combining Giddings' expression for the mean projected length with results presented in Happel and Brenner[10] for the effective hydro-
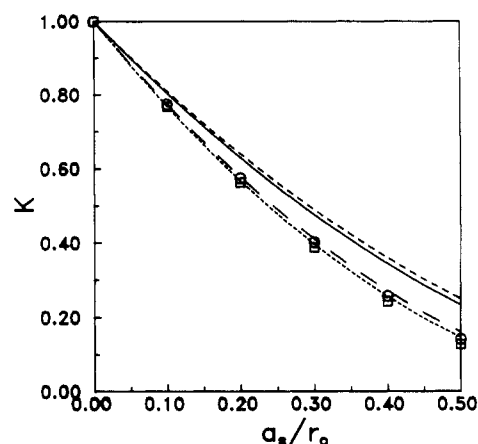

Figure 3. Partition coefficient values as a function of the ratio of hydrodynamic radius to pore radius: O, three-unit complex; □, eight-unit complex; —, oblate ellipsoid with axial ratio 0.5; — —, oblate ellipsoid with axial ratio 0.05; - - -, oblate ellipsoid with axial ratio <0.01; – –, spherical solute (eq 2).

dynamic radius of oblate ellipsoids, the following expression is obtained:

$$\frac{x_m}{r_0} = \frac{a_s}{r_0} \frac{\sin^{-1}(1-\epsilon^2)^{1/2}}{(1-\epsilon^2)^{1/2}} \left[\frac{\epsilon}{2} + \frac{\sin^{-1}(1-\epsilon^2)^{1/2}}{2(1-\epsilon^2)^{1/2}} \right] \qquad (10)$$

where x_m is one-half the mean projected length of the ellipsoid and ϵ is the axial ratio, defined as the ratio of the minor to major axis. If one assumes the mean projected length characterizes partitioning of all solutes, then an ellipsoid-shaped molecule will have the same partitioning characteristics as a sphere with the same mean projected length. For a sphere, x_m is the sphere radius. Therefore

$$K = \left(1 - \frac{x_m}{r_0}\right)^2 \qquad (11)$$

A comparison of the results for multisubunit structures and oblate ellipsoids with axial ratios of 0.05 and 0.5 is shown in Figure 3. For small ϵ ($\epsilon < 0.01$), the coefficient of a_s/r_0 in eq 10 approaches $\pi^2/8$. This limiting value is also shown in Figure 3. The K values for the multisubunit structures are comparable to those for oblate ellipsoids with an axial ratio ~ 0.01–0.05. This axial ratio is considerably smaller than what one might expect on the basis of the ratio of the smallest to largest dimension of the multisubunit structures. This ratio ranges from ~ 0.3 to 0.5.

An understanding of the relationship between equilibrium partitioning and solute size is important in the interpretation of elution behavior observed in size exclusion chromatography. Experimentally, the usual procedure is to prepare a calibration curve from known standards and to then use this calibration to determine molecular size (usually in terms of molecular weight) of another sample. The calibration curve is prepared as a semilog plot of molecular weight versus elution volume. For a homologous series of macromolecules, one expects a linear relationship between log molecular weight and elution volume. Such a relationship is expected only if the conformation of all samples used is the same because of the dependence of partitioning on molecular shape.

In our previously reported experimental study,[7,8] it was determined that the properties of the larger constituents of a heavy oil sample could be described by model complexes comprised of subunits whose size was that of the smallest constituents. That is, complexes with a constant value of σ (but with an increase in the number of subunits as molecular weight increased) were found to reasonably model the observed behavior of these materials. The re-
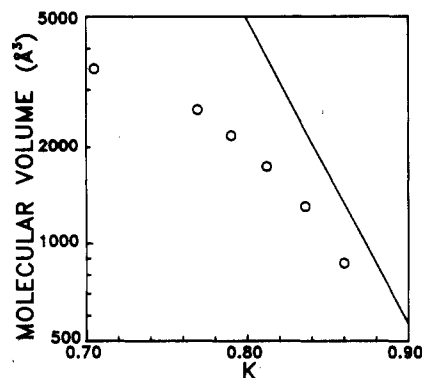
Figure 4. Molecular volume as a function of partition coefficient for complexes with $\sigma = 4.7$ Å and pore radius = 100 Å. Each data point corresponds to one of the structures in Figure 1. — corresponds to spherical solutes.

sults reported here can be used to investigate the type of calibration curve one can expect for a series of solutes which is modeled in this manner. Rather than molecular weight, molecular volume is plotted on the ordinate. Molecular volume is proportional to molecular weight with density and Avogadro's number included in the proportionality factor. The partition coefficient is plotted on the abscissa rather than elution volume. These values should also be proportional assuming only steric interactions are controlling the separation. A subunit size of 4.7 Å was chosen because this is the value we experimentally determined for the sample we investigated. A pore size of 100 Å was chosen because it is typical of size exclusion packings for solutes of this size. Figure 4 shows a semilog plot of volume versus K. The polynomial fit (eq 9 and Table II) for each geometry was used in determining K. For comparison, predictions for spherical solutes partitioning in the same size pore are also included. Figure 4 shows that there is a nonlinear relationship between log volume (or molecular weight) and K (or elution volume) for these structures. This observation is illustrative of the fact that molecular volume (or molecular weight) cannot be used to characterize partitioning for solutes with different molecular conformation, even for those with quite similar geometries. The difference between the calibration curve for the multisubunit structures and the spherical solutes provides further support for this statement. Figure 4 also demonstrates the errors that can be introduced if a calibration curve prepared by using one type of molecule is used to predict the molecular weight of a substance with a different conformation.

In obtaining these results, the integrals in eq 3 and 4 were approximated by using discrete segments in orientation and radial position. To determine the influence of this approach on the reported values of K, calculations were performed with different step sizes for the six-unit model with $a_s/r_0 = 0.2$. When the angular increment was varied from $\pi/10$ to $\pi/30$ (with 100 radial positions investigated), a difference of less than 1% in K was observed ($K = 0.5661$–0.5664). A similar insensitivity to the step size in radial position was also observed. When the number of radial positions was increased from 50 to 200 (with an angular increment of $\pi/20$), K was found to vary from 0.5661 to 0.5666. Therefore, this approximation to the integrals appears to be reasonable.

The motivation for this investigation was the desire to gain some understanding of the influence of solute conformation on partitioning of rigid, planar solutes. The results presented here will be useful for modeling exclusion and transport processes for heavy oil samples in porous media. In addition, these results may be useful in understanding and modeling the properties of polypropylene glycol. This polymer is used as a calibration standard for size exclusion chromatography. It has been demonstrated that this polymer takes on a rigid, disklike conformation under certain solvent conditions.[11] The approach presented here could also be applied to rodlike geometries, which may be used to model the structure of protein molecules.

References and Notes

(1) Giddings, J. C.; Kucera, E.; Russell, C. P.; Myers, M. N. *J. Phys. Chem.* **1968**, *72*, 4397.
(2) Casassa, E. F. *Macromolecules* **1976**, *9*, 182.
(3) Davidson, M. G.; Suter, U. W.; Deen, W. M. *Macromolecules* **1987**, *20*, 1141.
(4) Smith, F. G.; Deen, W. M. *J. Colloid Interface Sci.* **1980**, *78*, 444.
(5) Smith, F. G.; Deen, W. M. *J. Colloid Interface Sci.* **1983**, *91*, 57.
(6) Smith, F. G.; Deen, W. M. *J. Membr. Sci.* **1982**, *12*, 217.
(7) Kyriacou, K. C.; Baltus, R. E.; Rahimi, P. *Fuel* **1988**, *67*, 109.
(8) Kyriacou, K. C.; Sivaramakrishna, V. V.; Baltus, R. E.; Rahimi, P. *Fuel* **1988**, *67*, 15.
(9) Garcia de la Torre, J.; Bloomfield, V. A. *Biopolymers* **1978**, *17*, 1605.
(10) Happel, J.; Brenner, H. *Low Reynolds Number Hydrodynamics*; Martinus Nijhoff: The Hague, 1983; pp 205–206, 220–224.
(11) Sandell, L. S.; Goring, D. A. I. *Macromolecules* **1970**, *3*, 54.